Electronic Supplementary Information (ESI)

Silver Nanoparticle Functionalized Glass Fibers for Combined Surface-Enhanced Raman Scattering Spectroscopy (SERS) / Surface-Assisted Laser Desorption/Ionization (SALDI) Mass Spectrometry via Plasmonic /Thermal Hot Spots

Masahiro Kurita, Ryuichi Arakawa, and Hideya Kawasaki*

Department of Chemistry and Materials Engineering, Faculty of Chemistry, Materials and Bioengineering, Kansai University, 3-3-35 Yamate-cho; Suita-shi, Osaka 564-8680, Japan

*To whom correspondence should be addressed:

Hideya Kawasaki

Email: hkawa@kansai-u.ac.jp

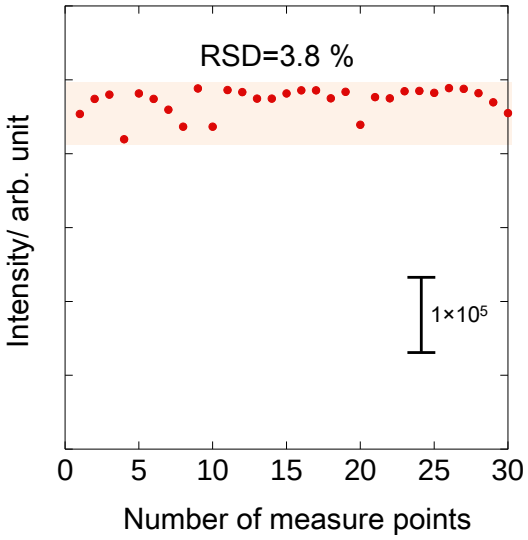

Figure S1 SERS peak intensities of 4-ATP at 1064 cm^{-1} on the Ag NP-GF substrates with 35 μg /cm^2 of Ag. The standard error obtained from 30 different locations is 3.8 % in the Raman signals. Before the SERS measurements, the Ag NP-GF substrates were immersed in 100 μM 4-ATP solution.

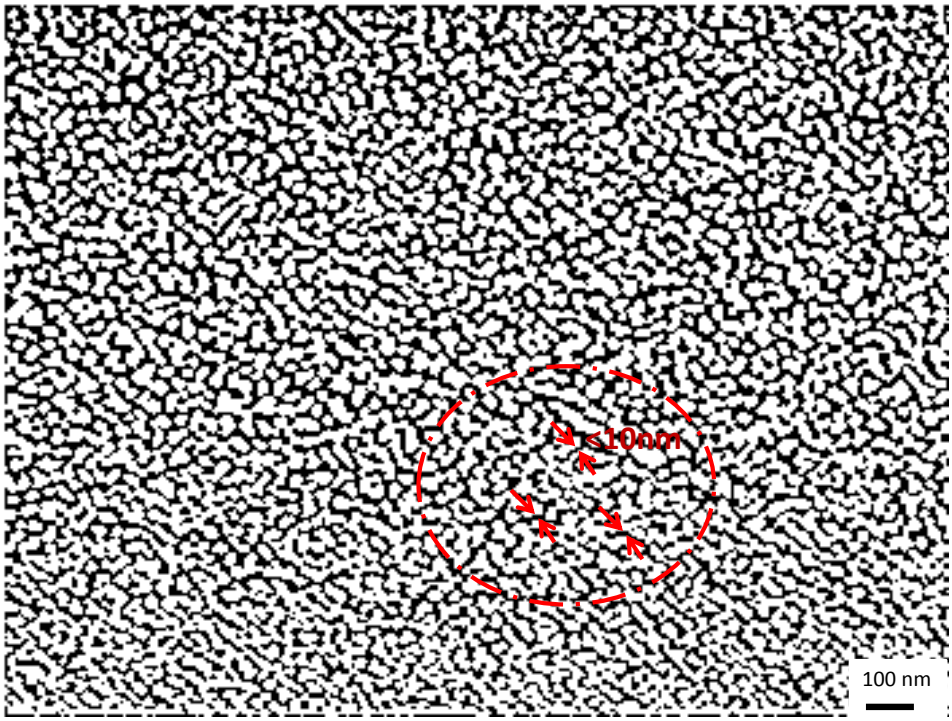

Figure S2 Binary image of the SEM image (Fig. 2b in the main text). We measured the inter-particle distance from the binary image and confirmed the presence of many inter-particle nanoscale gaps < 10 nm in the substrate as shown in red arrows in the figure.

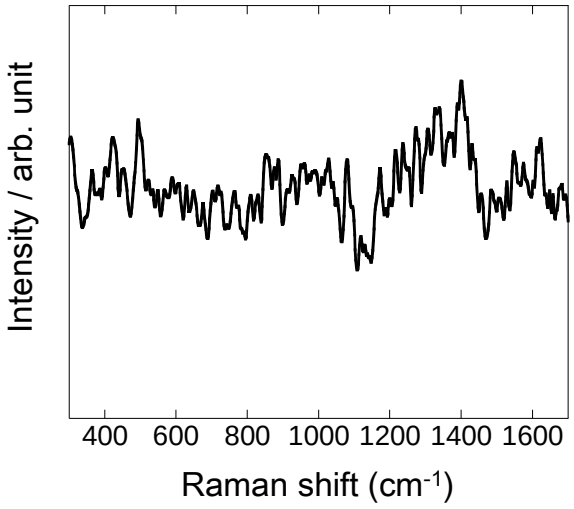

Figure S3. SERS spectrum of 4-ATP (1 μM) on the AgNP-functionalized glass "plate" with 35 μg/cm^2 Ag.

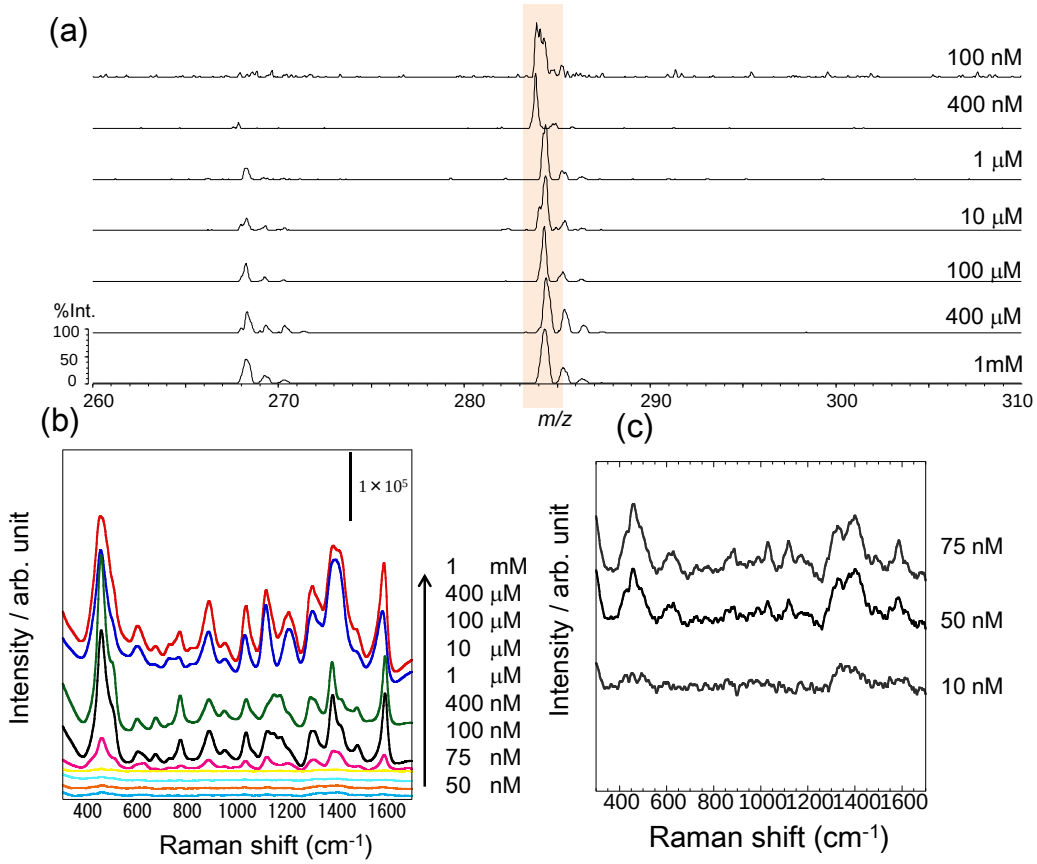

Figure S4. (a) SALDI mass spectra of MB on the Ag NP-GF substrate with 35 μg /cm^2 obtained from different concentrations of MB. (b), (c) SERS spectra of MB on the the Ag NP-GF substrate with 35 μg /cm^2 obtained from different concentrations of MB. Herein, the SALDI signal intensities of MB at *m/z* 284 $[M\text{-}Cl]^+$ and the Raman intensities of MB at 451 cm^{-1} were used in the evaluation of enhanced factors.

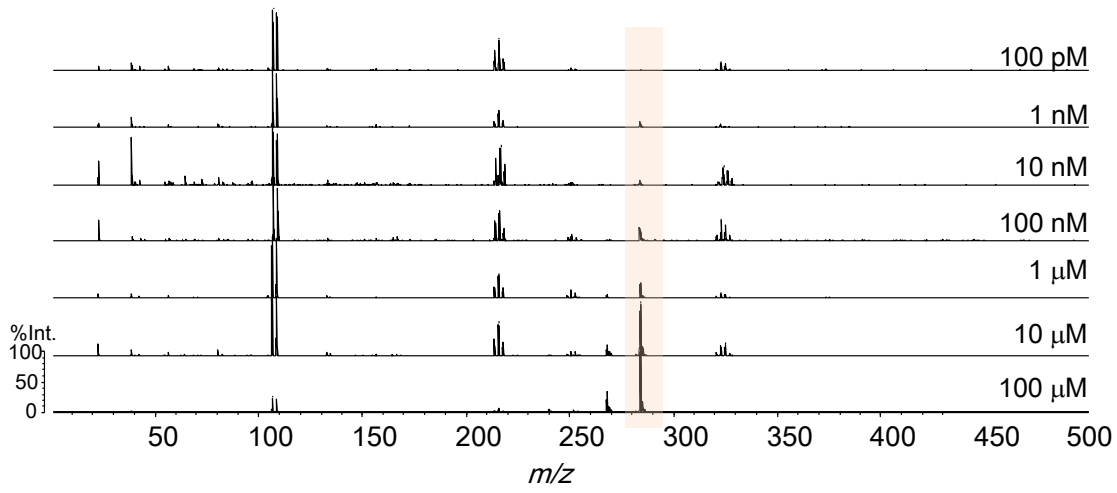

Figure S5 SALDI mass spectra of MB on the Ag NP-GF substrate with 35 μg /cm^2 obtained from different concentrations of MB.

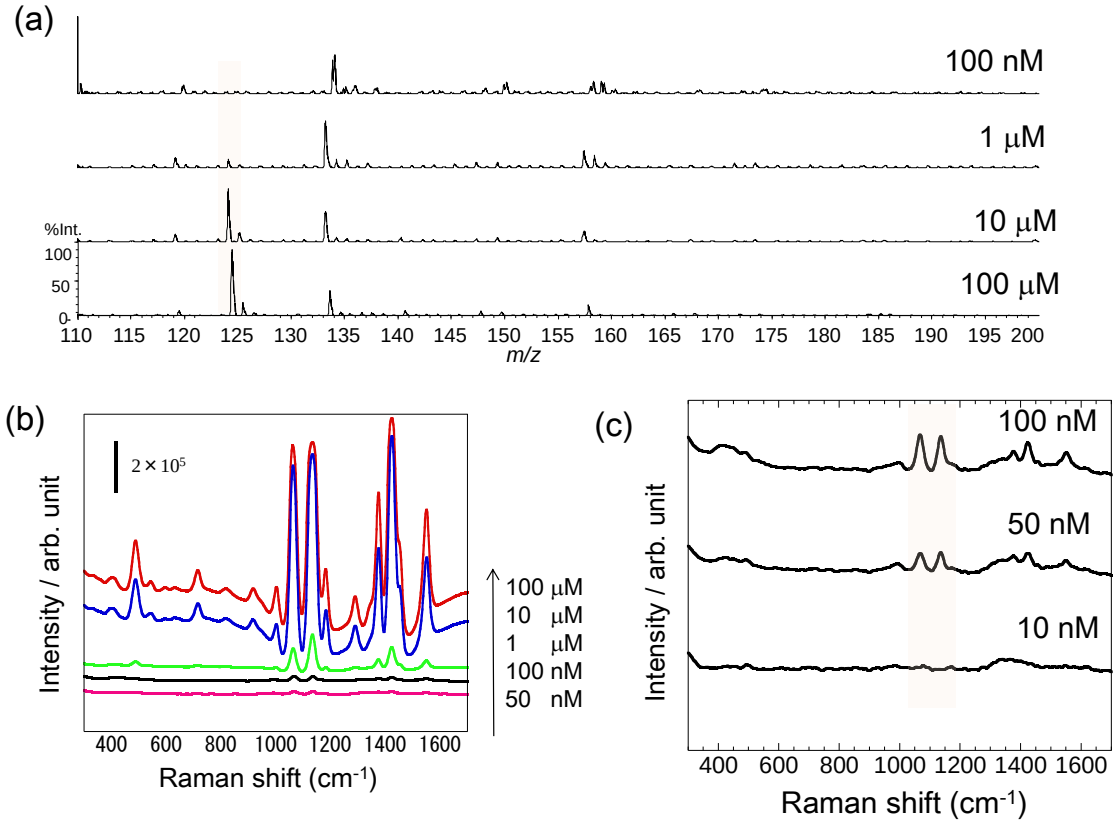

Figure S6. (a) SALDI mass spectra of 4-ATP on the Ag NP-GF substrate with 35 μg /cm^2 obtained from different concentrations of 4-ATP. (b), (c) SERS spectra of 4-AT P on the the Ag NP-GF substrate with 35 μg /cm^2 obtained from different concentrations of 4-ATP. Herein, the SALDI signal intensities of 4-ATP at *m/z* 124 $[M-H]^+$ and the Raman intensities of 4-ATP at 1066 cm^{-1} were used in the evaluation of enhanced factors.

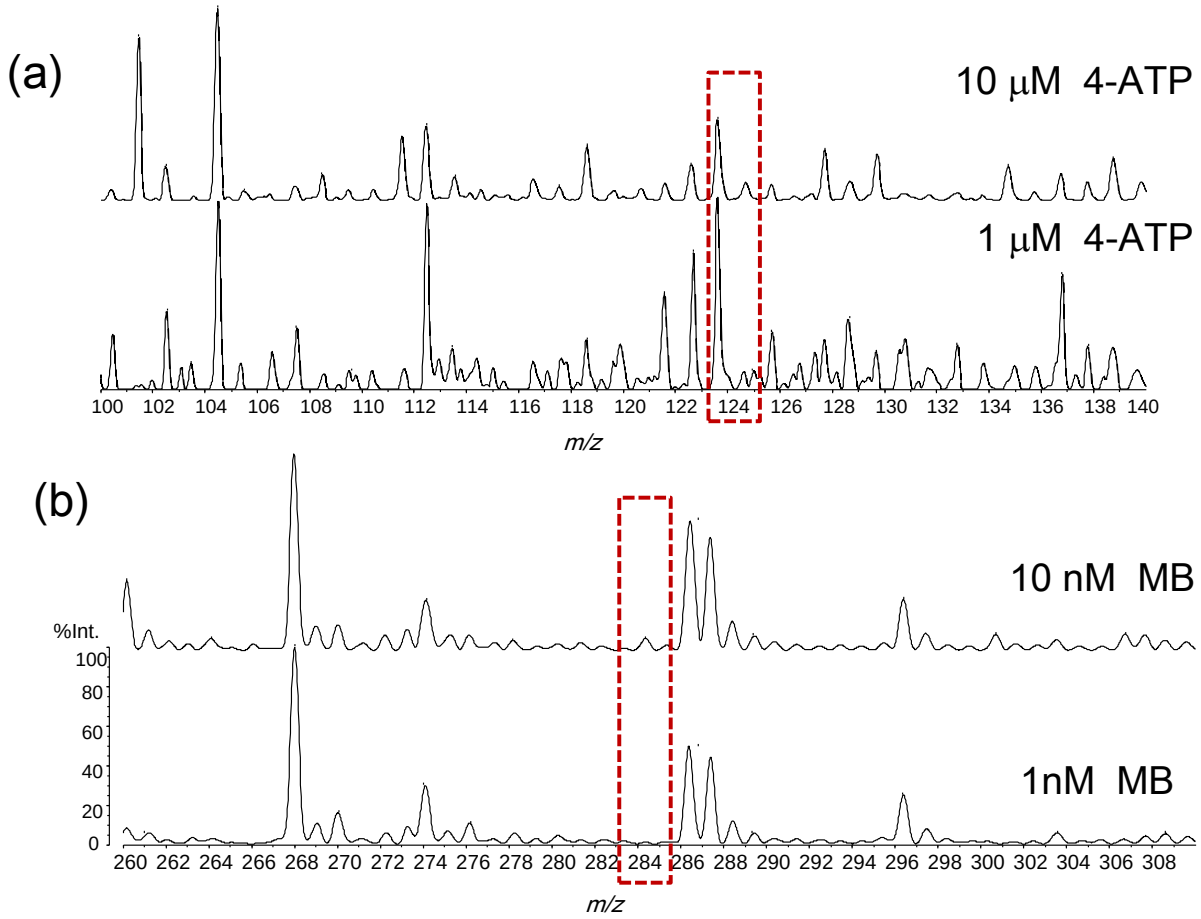

Figure S7. MALDI spectra of (a) 4-ATP and (b) MB on the bare glass fibers using CHCA matrix (10 mg/ mL). The peaks of 4-ATP ($[M-H]^+$ at *m/z* =124) and MB ([M-Cl] + at *m/z* 284) both were not detectable at the concentrations in the MALDI-MS.

Table 1. Peak Frequencies and Assignment for Neat 4-ATP and 4-ATP on the Ag-GF

Solid 4-ATP[a)]	Ag-GF 4-ATP	Assignment
1591(s)	1552(s)	νCC
1493(w)		
1425(vw)	1425(vs)	νCC+δCH
1369(vw)	1378(s)	δCH+νCC
	1292(w)	
1179(m)	1184(w)	δCH
1126(vw)	1136(vs)	δCH
1085(vs)	1066(vs)	νCS
1008(w)	1003(w)	γCC+γCCC
	714(vw)	
465(vs)	488(w)	γCCC
387(m)	409(vw)	δCS

Abbreviations: ν: stretching, δ: skeletal deformation, γ : out-of-plane bending,
vs: very strong, s: strong, w : weak, vw : very weak
a) Ref. 28 in the text.

Table 2. Peak Frequencies and Assignment for Neat MB and MB on the Ag-GF

Solid MB[b)]	AG-GF MB	Assignment
1618(s)		ν(CC)ring
	1592(s)	ν(CC)ring
1544(w)		ν_{asym}(CC)
1441(w)	1480(w)	ν_{asym}(CN)
1396(m)	1381(s)	α (CH)
1331(w)	1309(m)	
1272(w)		
1181(m)	1173(w)	ν(CH)
1067(w)		
	1035(m)	β(CH)
	949(w)	
	885(m)	
768(w)	770(m)	
677(w)	669(w)	γ(CH)
	600(w)	δ(CSC)
497(w)		δ(CNC)
445(s)	451(s)	δ(CNC)

Abbreviations: s:strong, m:medium, w: weak; ν:stretching, α:in-plane ring deformation,
β:in-plane bending, γ: out-of-plane bending and δ:skeletal deformation.
b) Ref. 36 in the text.